Roy, Sonali and Robson, Fran and Lilley, Jodi and Liu, Cheng-Wu and Cheng, Xiaofei and Wen, Jiangqi and Walker, Simon and Sun, Jongho and Cousins, Donna and Bone, Caitlin and Bennett, Malcolm J. and Downie, J. Allan and Swarup, Ranjan and Oldroyd, Giles and Murray, Jeremy D. (2017) MtLAX2, a functional homologue of the Arabidopsis auxin influx transporter AUX1, is required for nodule organogenesis. Plant Physiology, 174 (1). pp. 326-338. ISSN 1532-2548

[AU : QA1]

MtLAX2, a Functional Homologue of the Arabidopsis Auxin Influx Transporter AUX1, Is Required for [AU : 1] Nodule Organogenesis[1]

Sonali Roy, Fran Robson, Jodi Lilley, Cheng-Wu Liu, Xiaofei Cheng, Jiangqi Wen, Simon Walker, Jongho Sun, Donna Cousins, Caitlin Bone, Malcolm J. Bennett, J. Allan Downie, Ranjan Swarup, Giles Oldroyd, and Jeremy D. Murray*

Department of Cell and Developmental Biology, John Innes Centre, Norwich Research Park, Norwich, NR4 7UH, United Kingdom (S.R., F.R., J.L., C.-W.L., J.S., D.C., C.B., G.O., J.D.M.); Plant Biology Division, Samuel Roberts Noble Foundation, 2510 Sam Noble Parkway, Ardmore, Oklahoma 73401 (S.R., J.W.); Department of Molecular Microbiology, John Innes Centre, Norwich Research Park, Norwich, NR4 7UH, United Kingdom (S.W., J.A.D.); Plant and Crop Science Division, School of Biosciences, University of Nottingham, Nr Loughborough LE12 5RD, United Kingdom (M.J.B., R.S.); and Babraham Institute, Babraham Hall, Babraham CB22 3AT, United Kingdom (S.W.)

ORCID IDs: 0000-0003-2734-5124 (S.R.); 0000-0002-6650-6245 (C.-W.L.); 0000-0001-5113-7750 (J.W.); 0000-0001-9185-4922 (S.W.); 0000-0002-3705-3072 (J.S.); 0000-0003-2527-8896 (D.C.); 0000-0002-5881-3202 (C.B.); 0000-0003-0475-390X (M.J.B.); [AU : 3] **0000-0003-1011-4960 (J.A.D.); 0000-0002-6438-9188 (R.S.); 0000-0003-3000-9199 (J.D.M.).**

Most legume plants can form nodules, specialized lateral organs that form on roots, and house nitrogen-fixing bacteria collectively called rhizobia. The uptake of the phytohormone auxin into cells is known to be crucial for development of lateral roots. To test the role of auxin influx in nodulation we used the auxin influx inhibitors 1-naphthoxyacetic acid (1-NOA) and 2-NOA, which we found reduced nodulation of *Medicago truncatula*. This suggested the possible involvement of the AUX/LAX family of auxin influx transporters in nodulation. Gene expression studies identified *MtLAX2*, a paralogue of Arabidopsis (*Arabidopsis thaliana*) *AUX1*, as being induced at early stages of nodule development. *MtLAX2* is expressed in nodule primordia, the vasculature of developing nodules, and at the apex of mature nodules. The *MtLAX2* promoter contains several auxin response elements, and treatment with indole-acetic acid strongly induces *MtLAX2* expression in roots. *mtlax2* mutants displayed root phenotypes similar to Arabidopsis *aux1* mutants, including altered root gravitropism, fewer lateral roots, shorter root hairs, and auxin resistance. In addition, the activity of the synthetic DR5-GUS auxin reporter was strongly reduced in *mtlax2* roots. Following inoculation with rhizobia, *mtlax2* roots developed fewer nodules, had decreased DR5-GUS activity associated with infection sites, and had decreased expression of the early auxin responsive gene *ARF16a*. Our data indicate that MtLAX2 is a functional analog of Arabidopsis AUX1 and is required for the accumulation of auxin during nodule formation in tissues underlying sites of rhizobial infection.

INTRODUCTION

Legume plants form a symbiotic relationship with a group of soil bacteria called rhizobia, leading to the formation of specialized root organs called nodules. Within the nodules, the rhizobia are taken up into the cells where they reduce atmospheric nitrogen to ammonia, which promotes plant growth and productivity. Several previous studies have indicated an important role for the plant hormone auxin in nodule formation. We show that chemical inhibitors of auxin uptake reduced nodulation in the model legume *Medicago truncatula*. We studied the gene expression of the auxin influx carrier AUX/LAX family in *M. truncatula* and found that one member, *MtLAX2*, showed increased expression at the very early stages of nodule formation. Comparison of *MtLAX2* with other *LAX* genes indicated that it is the counterpart of *AUX1*, a gene that has been shown to be involved in root branching in the nonlegume Arabidopsis (*Arabidopsis thaliana*). *M. truncatula* mutants with a defective *MtLAX2* gene showed reduced responses to auxin and had fewer lateral roots and nodules compared to wild-type plants. Our findings indicate that MtLAX2-mediated auxin accumulation is important for nodule formation in legumes.

[1] This work was supported by BBSRC awards BB/G023832/1 and BB/L010305/1 and the John Innes Foundation.

* Address correspondence to jeremy.murray@jic.ac.uk.

The author responsible for distribution of materials integral to the findings presented in this article in accordance with the policy described in the Instructions for Authors (www.plantphysiol.org) is: [AU : 2] Jeremy Murray (jeremy.murray@jic.ac.uk).

J.D.M. and S.R. designed and supervised the experiments; the majority of experiments were performed by S.R. with contributions from F.R., J.L., C.-W.L., J.S., D.C., C.B., S.W., R.S., X.C.; J.W.; S.R., J.D.M., J.A.D., G.E.D., R.S., and M.B. wrote the article.

www.plantphysiol.org/cgi/doi/10.1104/pp.16.01473

Plants integrate internal developmental cues and environmental signals to regulate root growth including the production of lateral roots for anchoring in the soil and nutrient foraging. One example of this is the formation of lateral roots in response to low nitrogen availability. The formation of lateral roots is governed by the growth hormone auxin at every stage (Lavenus et al., 2013). In Arabidopsis, oscillations in auxin signaling in the basal root meristem are correlated with future sites of lateral root emergence suggesting that initiation sites are "primed" (De Smet et al., 2007). Moreover, localized auxin signaling precedes, and is required for, the initial divisions of lateral root founder cells in the pericycle (De Smet et al.2007; Dubrovsky et al., 2008; Laskowski et al., 2008). Both initiation and subsequent emergence of lateral roots is associated with localized increases in auxin concentration, which depend on members of the AUX-LAX family of auxin influx transporters (Marchant et al., 2002; Swarup et al., 2008; Swarup and Péret, 2012). A second example of root developmental responses conditioned by plant nutrient status is nodulation. Nodules are specialized lateral organs that form on roots of legumes and actinorhizal plants during symbiosis with nitrogen-fixing soil bacteria. Despite gross functional and anatomical differences, lateral roots and nodules possess some common features: cell divisions in the pericycle occur during their formation (Malamy and Benfey, 1997; Timmers et al., 1999; Lucas et al., 2013; Xiao et al., 2014); both lateral roots and indeterminate nodules feature a persistent meristem, and both organ types initiate opposite protoxylem poles, a phenomenon that, at least for nodulation, depends on ethylene signaling (Heidstra et al., 1997; Casimiro et al., 2001; Penmetsa et al., 2003; Lohar et al., 2009). Nevertheless, important differences exist: in nodule development, the pericycle divisions are accompanied by divisions in the cortex. These cortical divisions give rise to the majority of the cells in mature nodules, whereas lateral roots are comprised mainly of pericycle-derived cells (Xiao et al., 2014; Herrbach et al., 2014; de Billy et al., 2001). Developing lateral roots possess a centrally located vasculature while legume nodules develop multiple vascular strands on the periphery of the nodule (Guan et al., 2013). Interestingly, actinorhizal nodules, which are evolutionarily more ancient than legume nodules, feature a central vasculature (Péret et al., 2007). Furthermore, knockdown of several *M. truncatula PLETHORA* family members, encoding transcription factors that have been linked to auxin biosynthesis in Arabidopsis (Aida et al., 2004; Pinon et al., 2013; Yamaguchi et al., 2016), reduced nodulation and impaired nodule-meristem function in *M. truncatula* (Franssen et al., 2015). Based on these observations we can predict further overlap in the genes involved in the formation of nodules and lateral roots, but that different timing, levels, and location of expression of these genes will be important in determining which lateral organ is formed.

To date, studies on the hormonal regulation of nodule development have mainly focused on cytokinin auxin and ethylene, which can act as either positive or negative regulators of nodulation (for review, see Miri et al., 2016; Guinel, 2015). In particular, cytokinin signaling has been shown to be both necessary and sufficient for nodule formation, being required for the timely division of cortical cells leading to primordia formation (Murray et al., 2007; Tirichine et al., 2007; Gonzalez-Rizzo et al., 2006). Studies using various markers indicate that increased auxin signaling occurs at the site of nodule primordium formation in determinate and indeterminate nodules and in meristems of indeterminate nodules (Mathesius et al., 1998; Pacios-Bras et al., 2003; Suzaki et al., 2012, 2013; Breakspear et al., 2014; Roux et al., 2014). In addition, transcripts of members of the *AUX/LAX* gene family, which encode auxin influx transporters, are expressed in nodule primordia (de Billy et al., 2001). Furthermore, physiological studies of the hypernodulated mutants *sunn* and *sickle* revealed that increased nodulation in these mutants is correlated with increases in auxin transport rates and auxin content of roots (Prayitno et al., 2006; van Noorden et al., 2006). Despite this large and growing body of circumstantial evidence implicating auxin in nodulation, relatively few functional studies have been carried out. Application of auxin transport inhibitors to roots can induce formation of "pseudonodules" on some legumes and RNAi silencing in *M. truncatula* of a set of *PIN* genes, which encode auxin efflux transporters, supports a role for changes in auxin distribution in nodule formation (Allen et al., 1953; Hirsch et al., 1989; Rightmyer and Long, 2011; Huo et al., 2006). While progress has been made, our understanding of the role of auxin in nodulation is limited and has been hindered by the lack of available auxin signaling and transport mutants. Here we characterize the role of *MtLAX2*, a functional analog of the auxin influx transporter *AtAUX1*. We report that *mtlax2* mutants are compromised in nodulation, indicating a role for auxin influx in nodule formation in legumes.

RESULTS

Auxin Transport Inhibitors Block Nodule Development but Not Nod-Factor Signaling

To investigate the importance of influx transporter-driven auxin movement in nodulation, we used the auxin transport inhibitors 1-naphthoxyacetic acid (1-NOA) and 2-NOA, which, at low concentrations, can block auxin entry into plant cells, but do not themselves act as auxins (Delbarre et al., 1996). *M. truncatula* A17 seedlings pretreated for 24 h with 1-NOA or 2-NOA were inoculated with *Sinorhizobium meliloti* (Rm2011) and then allowed to grow for 7 d. Both 1-NOA and 2-NOA decreased the total number of nodules by 50% (Fig. 1A, left) and also decreased primary root length (Supplemental Fig. S1A). Reduction in nodule numbers

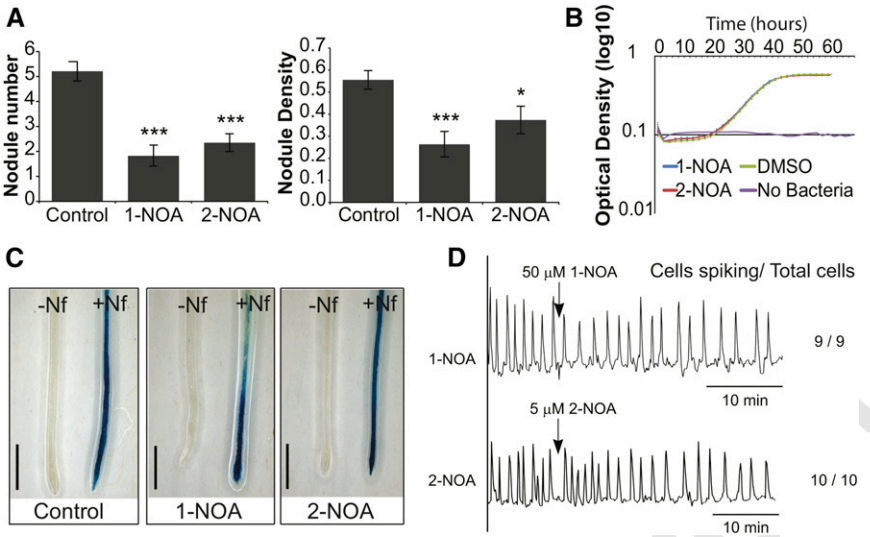

Figure 1. Inhibiting auxin influx affects nodule numbers but not Nod factor signaling. A, Average nodule number (left) and nodule density (right) on *M. truncatula* seedlings grown in the constant presence of auxin influx inhibitors, either 50 μM 1-NOA or 5 μM 2-NOA, 7 dpi with *S. meliloti* (Rm2011). $n = 19, 17, 20$ for control, 1-NOA, and 2-NOA, respectively. Student's *t* test $^{***}P < 0.001$ and $^{*}P < 0.01$. Error bars depict SEM. B, Growth of Rm2011 in presence of 1-NOA and 2-NOA at the above concentrations. Bars depict SEM. C, Representative images showing staining of *M. truncatula* seedlings carrying the *ENOD11*$_{pro}$*-GUS* reporter after 24 h pretreatment with 50 μM 1-NOA and 5 μM 2-NOA with or without 1 μM Nod factor (NF) treatment for an additional 24 h. Scale bar 800 μm. D, Calcium oscillations initiated in root hairs of *M. truncatula* seedlings treated with 1 μM Nod factor with addition of 50 μM 1-NOA or 5 μM 2-NOA. Numbers of root hairs testing positive for calcium spiking after treatment are indicated to the right.

was not simply a consequence of having shorter roots, as nodule density was also reduced compared to control seedlings (Fig. 1A, right). The growth of *S. meliloti* Rm2011 was unaffected by the presence of these auxin transport inhibitors (Fig. 1B).

Since nodule organogenesis requires the Nod factor signaling pathway, we tested whether auxin transport inhibitors interfere with signal transduction thereby affecting nodule initiation. First, we tested whether the symbiotic marker gene *ENOD11* was activated by Nod factors in the presence of these auxin transport inhibitors. Three-day-old *ENOD11*$_{pro}$*-GUS* transgenic seedlings pretreated for 24 h with 1-NOA or 2-NOA were transferred to a fresh solution containing the auxin transport inhibitor and 1 nM Nod factors for an additional 24 h. GUS staining of these seedlings revealed that 1-NOA and 2-NOA did not block induction of *ENOD11* (Fig. 1C). Next, we checked whether Nod factor-induced calcium spiking was affected; calcium oscillations induced by 1 nM Nod factor were not affected by either 1-NOA or 2-NOA (Fig. 1D). We also tested effects of indole-3-acetic acid (IAA) and the auxin efflux transport inhibitor, 1-naphthylphthalamic acid (NPA) and found that both reduced nodule numbers (Supplemental Fig. S1B). Neither IAA nor NPA inhibited *ENOD11* gene activation or perturbed Nod factor-induced calcium oscillations (Supplemental Fig. S1, C and D). Neither IAA nor NPA affected the growth of *S. meliloti* in liquid culture (Supplemental Fig. S1E). These results suggest that Nod factor signaling is not affected by auxins and auxin transport inhibitors and therefore inhibition of auxin influx may directly affect nodule development.

MtLAX2, a Paralogue of the Auxin Importer *AtAUX1*, Is Induced by *S. meliloti*

We investigated the expression of the AUX-LAX family of auxin influx transporters in *M. truncatula* root segments spot inoculated with rhizobia (Rm2011). The MtLAX family comprises five genes (described by Schnabel and Frugoli, 2004) and the expression of one member, *MtLAX2* (Medtr7g067450), was the only *LAX* gene significantly upregulated 16 h after inoculation compared to mock inoculated roots (Fig. 2A). Phylogenetic analysis indicates that MtLAX2 is paralogous to Arabidopsis AUX1 (Fig. 2B) and that it is most closely related to AtAUX1, as was previously reported by Schnabel and Frugoli (2004). This was confirmed by comparison of the chromosomal regions containing *MtLAX2* to Arabidopsis, which revealed extensive microsynteny to the *AtAUX1* and *AtLAX2* regions (Supplemental Fig. S2).

Next, we investigated the spatial expression patterns of *MtLAX2* in roots using the *MtLAX2* promoter driving the GUS reporter. This revealed that like *AtAUX1*, *MtLAX2* is expressed in the root meristem, lateral root primordia, and vascular bundles of uninfected roots (Supplemental Fig. S3, A–D). Upon infection with *S. meliloti*, we found that *MtLAX2* expression was associated with proliferative cell divisions subtending sites of

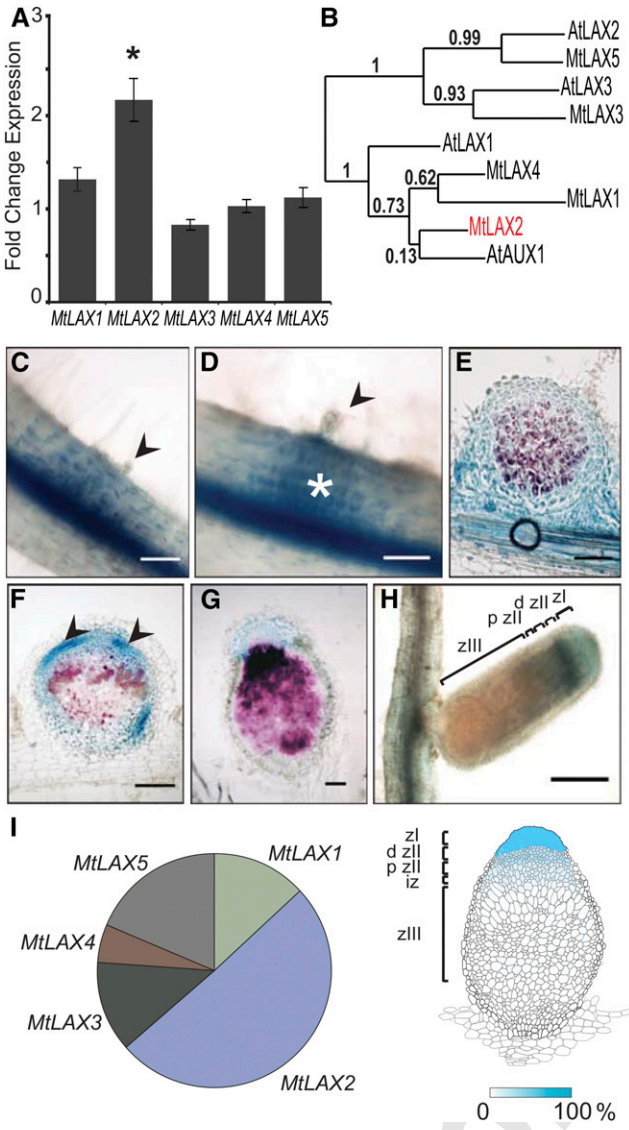

Figure 2. *LAX* gene expression is associated with nodule formation. A, qRT-PCR data showing expression of members of the AUX-LAX family of genes in root segments of *M. truncatula* 16 h postinoculation with *S. meliloti* (Rm2011) compared to mock (16 h posttreatment). Expression is relative to *EF1α* and data are the average of five biological replicates. Student's *t* test $*P \leq 0.01$. Bars depict SEM. B, Phylogram of the *M. truncatula* and Arabidopsis AUX-LAX proteins. Branch labels are likelihood support values. C to H, GUS stained *MtLAX2pro-GUS* expressing hairy roots of *M. truncatula* during early infection (C), in a nascent nodule primordium (D), in a thin section of a young nodule (E), in a thin section of a developing nodule 2 wpi (F), and in a thin section of 4 wpi (G) or whole mount of 5 wpi mature nodules (H). Infected root hair cells are indicated by arrowheads in C and D. Dividing cells of the nodule primordium are indicated by an asterisk in D. Vascular bundles are indicated by arrowheads in F. *S. meliloti* was stained in magenta (E–G). I, Left side: Relative expression of different LAX family members in *M. truncatula* nodules. Data from Roux et al. (2014). Right side: Diagram represents the percentage of the total normalized RNAseq reads of all LAX family members (*MtLAX1*, *MtLAX2*, *MtLAX3*, *MtLAX4*, *MtLAX5*) in each nodule zone as reported by Roux et al. (2014). d zII, distal zone II; iz, interzone; p zII, proximal zone II; zI, zone I; z III, zone III of an indeterminate nodule. Scale bars 100 μm (C–G), 1,000 μm (H).

apparently successful infections (Fig. 2, C and D). However, not every root hair undergoing infection or curling in response to *S. meliloti* was associated with underlying cortical $MtLAX2_{pro}$-GUS expression. This may be due to the fact that during nodulation many infections are aborted, or could simply reflect inconsistency of *MtLAX2* expression in early nodule development. GUS staining was high throughout the nodule primordium (Fig. 2E), and the nodule vascular bundles (Fig. 2F), before becoming exclusively confined to the nodule apex 5 weeks after inoculation (Fig. 2, G and H). Previous transcriptomic work using laser capture microdissection of mature *M. truncatula* nodules reported expression of several *AUX-LAX* genes in the dividing cells of the nodule apex (i.e. the meristem and distal infection zone), with *MtLAX2* being the most highly expressed family member, accounting for 51% of total LAX family normalized RNAseq reads (Fig. 2I). Another transcriptomic study using purified root hairs from rhizobially inoculated roots found that none of the *LAX* genes were significantly induced before or during infection (Breakspear et al., 2014; Supplemental Fig. S3E). [AU : 4]

Isolation of *mtlax2* Mutants

Using the *Tnt1* retrotransposon insertion population available for *M. truncatula* we screened for lines containing insertions in *MtLAX2*. The gene structure of *MtLAX2* is highly similar to that of *AtAUX1*, having eight exons (Fig. 3A). We identified two lines with independent insertions in exon four (Fig. 3A), which we designated *mtlax2-1* (NF14494) and *mtlax2-2* (NF16662). Sequencing of the *Tnt1* insertion sites confirmed that *mtlax2-1* and *mtlax2-2* have insertions at 1,144 and 1,242 bps downstream of the ATG start codon, respectively. *MtLAX2* expression was tested in homozygous mutants using semiquantitative RT-PCR. Full-length [AU : 5] transcripts could not be detected at 22 PCR cycles (Fig. 3B) in either mutant line. At higher cycle numbers using a *Tnt1*-specific primer and a gene-specific primer, weak bands were produced, confirming that the *MtLAX2* mRNAs are interrupted by *Tnt1* sequences in each case (Supplemental Fig. S4A). Sequencing of these products indicates that in both cases the different *Tnt1* insertions result in aberrant splicing creating premature stop codons (Supplemental Fig. S4, B and C) generating the same truncated protein. The transcripts produced would encode proteins missing several transmembrane regions that are present in the amino acid transport domain (Supplemental Fig. 4D). These findings indicate that *mtlax2-1* and *mtlax2-2* are very likely null mutants.

MtLAX2 Is a Functional Analog of AUX1 [AU : 6]

Mutations in *aux1* in Arabidopsis cause development of fewer lateral roots, agravitropic growth in roots, and shorter root hairs (Marchant et al., 2002; Bennett et al.,1996; Pitts et al., 1998; Rahman et al., 2002). To test

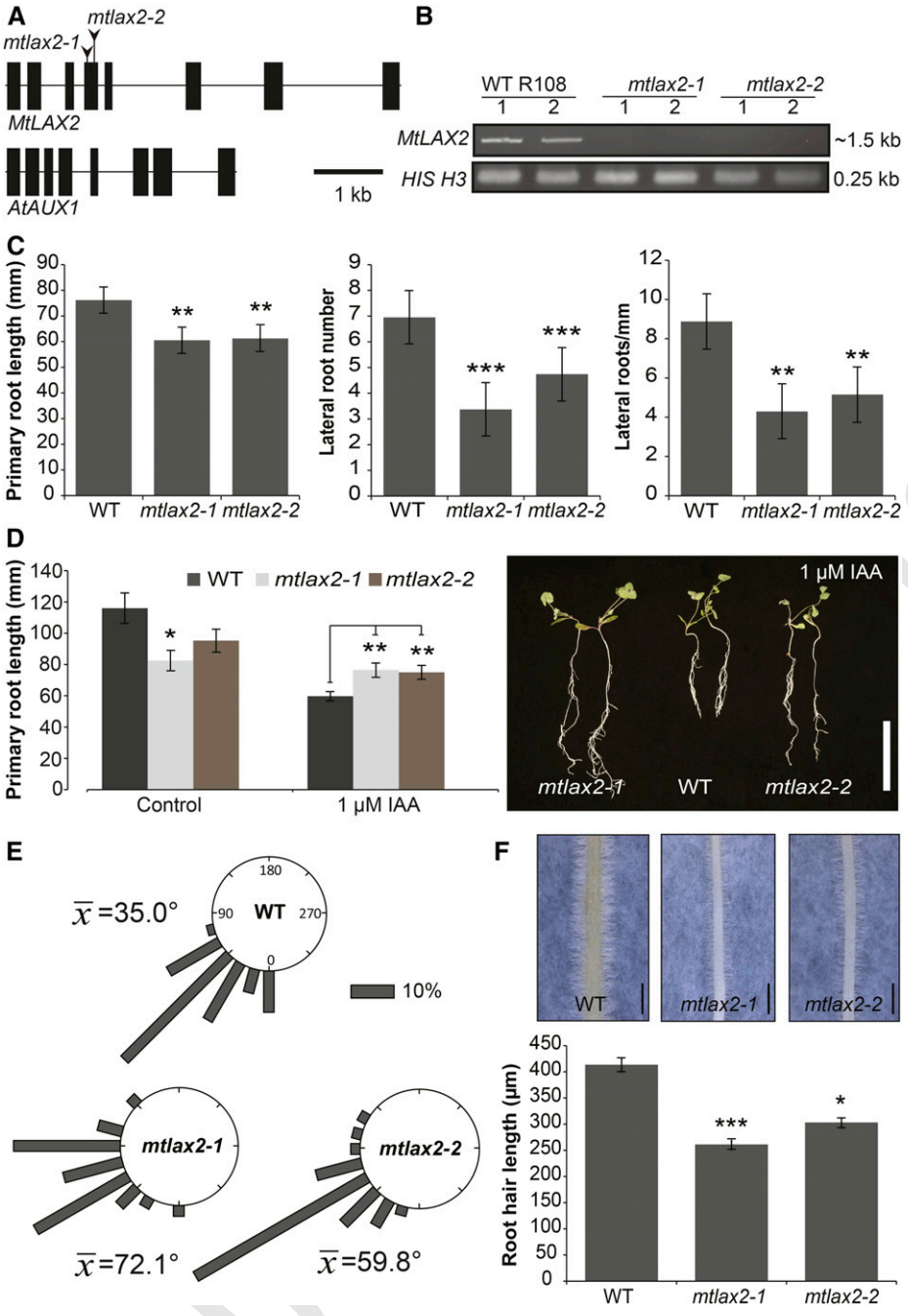

Figure 3. Identification and characterization of *M. truncatula mtlax2* mutants. A, *MtLAX2* gene structure is comprised of eight exons. The positions of the *Tnt1* retrotransposon insertions in *MtLAX2* are indicated (*mtlax2-1*: 1,144 bp and *mtlax2-2*: 1,242 bp). B, top: image of an agarose gel showing results of semi-quantitative RT-PCR (22 cycles) using *MtLAX4*-specific primers on cDNA generated from leaf tissue-extracted RNA of two different plants per line. bottom: gel image showing amplification of *Histone H3* cDNA from all samples. C, One week postgermination, *mtlax2* mutants have decreased primary root length (left), fewer lateral roots (middle), and decreased density of lateral roots per mm root length (right). Student's *t* test $^{**}P < 0.01$, $^{***}P < 0.001$. $n = 20, 15, 21$ for wild type (WT), *mtlax2-1*, and *mtlax2-2*, respectively. Bars depict SEM. D, left: *mtlax2* mutants show auxin-insensitive root growth 2 weeks after growth in soil with 1 μM IAA. Student's *t* test $^{*}P < 0.05$, $^{**}P < 0.01$. Error bars depict SEM. $n = 15–20$. right: representative image of the IAA-treated plants. E, Gravitropic responses in wild-type (WT) and *lax2* mutants 48 h post 90° stimulus. Length of the bar represents percentage of plants in each group. $n = 40$, 30, and 38 for wild type, *mtlax2-1*, and *mtlax2-2* respectively. Mean root growth angles are indicated. F, Root hair length in 10-d-old wild-type and *mtlax2* mutant seedlings. Representative images of root hairs in comparable root zones are shown above histograms showing average root hair length in the mature root zone. Student's *t* test $^{*}P < 0.05$, $^{**}P < 0.01$, $^{***}P < 0.001$. $n = 5$ seedlings per genotype and 10 root hairs per seedling. Error bars depict SEM.

if *mtlax2* mutations cause similar phenotypes, wild-type and *mtlax2* mutant seedlings were grown for 7 d in soil to compare root phenotypes. The *mtlax2* mutants had shorter primary roots, fewer lateral roots, and a 50% reduction in lateral root density (Fig. 3C). The *mtlax2* mutants were also insensitive to root growth inhibition by auxin when watered with 1 μM IAA for 2 weeks (Fig. 3D). Gravitropic responses measured 48 h post a 90° gravistimulus were compromised in the *mtlax2* mutants, which had increased growth angles (mean = 60–72°) compared to wild type (mean = 35°; Fig. 3E; *t* tests, $P < 1 \times 10^{-6}$). Root hair length, scored on 10-d-old seedlings, was reduced by 25% to 30% in the *lax* mutants (Fig. 3F).

Given that the *mtlax2* mutant phenocopies many of the *aux1* root defects, we next attempted to complement the *Arabidopsis aux1* mutant using *MtLAX2* expressed from the *AtAUX1* promoter. Forty independent transgenic lines carrying $AtAUX1_{pro}$-*MtLAX2* were isolated, but none recovered wild-type gravitropic responses or sensitivity to the synthetic auxin 2,4-dichlorophenoxyacetic acid (2,4-D; Supplemental Fig. S5), despite having stable expression of the transgene (Supplemental Fig. S6). [AU : 7]

MtLAX2 Is Required for Nodulation but Not Arbuscular Mycorrhization

As *MtLAX2* was highly expressed during root nodulation (Fig. 2), we also investigated whether *mtlax2* mutants exhibited nodule developmental defects. One week postinoculation (wpi) with rhizobia the number of nodules was reduced by one-half in both *mtlax2-1* and *mtlax2-2* mutants grown in soil (Fig. 4A). The average number of nodules was also reduced in *mtlax2* mutants grown on plates (Supplemental Fig. S7A, left) and this was correlated with a reduction in nodule density (Supplemental Fig. S7A, right), suggesting that the reduced nodulation in the mutant was not simply a consequence of reduced root length. A time course experiment using soil-grown plants revealed that the reduction in nodulation was significant 1 and 3 wpi but not at 4 wpi (Fig. 4B). Tests of nodulation in a segregating population of *mtlax2-2* revealed that at 2 wpi, plants homozygous for *mtlax2-2* had reduced nodulation, whereas heterozygotes and plants wild type for *LAX2* were indistinguishable from the wild-type control (Fig. 4C); this demonstrates that the *mtlax2*-2 mutation is recessive and that *MtLAX2* facilitates optimum nodule formation.

Four wpi those nodules formed on the *mtlax2* mutant appeared morphologically wild type-like, that is were elongated and pink (Supplemental Fig. S7B). Similarly, longitudinal sections through the cortex of *mtlax2* nodules (2 wpi) revealed wild type-looking symbiosomes and typical infection threads (Supplemental Fig. S7C), suggesting establishment of functional nitrogen fixation in the mutants. The expression of *MtLAX2-GUS* at the nodule apex (Fig. 2, G and H) suggested a potential role in nodule growth. To test this, we measured nodule length at 2 wpi and found that it was reduced in *mtlax2* mutant lines (Fig. 4D). Hence, *MtLAX2* appears to be required to facilitate nodule elongation, in addition to formation.

Much of the molecular machinery required for establishing nodulation and arbuscular mycorrhization is shared, and auxin has recently been implicated in interactions with arbuscular mycorrhiza (Hanlon and Coenen, 2011). To address this possibility, we tested the ability of the *mtlax2-1* mutant to be colonized by arbuscular mycorrhizal fungi and found that it was wild type-like (Supplemental Fig. S7D). Hence, *MtLAX2* appears to not be required to facilitate arbuscular mycorrhization.

MtLAX2 Is Auxin Inducible and Is Required for Auxin Signaling in the Root

Many genes involved in nodulation are induced by purified Nod factors, but published data indicate that no members of the AUX-LAX family are induced by Nod factors, suggesting that the induction of *MtLAX2* by *S. meliloti* might be indirect (Breakspear et al., 2014).

In silico analysis of the 2-kb upstream promoter region of the *MtLAX2* gene revealed the presence of three TGTCTC auxin responsive elements and two truncated TGTCT motifs (Fig. 5A) that the AUXIN RESPONSIVE FACTOR (ARF) family of transcription factors have been shown to bind (Ulmasov et al., 1999; Walcher and Nemhauser, 2012). To test whether *MtLAX2* is auxin-inducible, we treated *M. truncatula* seedlings with either 1 μM IAA or its structural analog benzoic acid and monitored *MtLAX2* gene expression using quantitative RT (qRT)-PCR. IAA, but not benzoic acid or the dimethyl sulfoxide carrier, strongly increased the expression of *MtLAX2* (Fig. 5B). To determine whether the

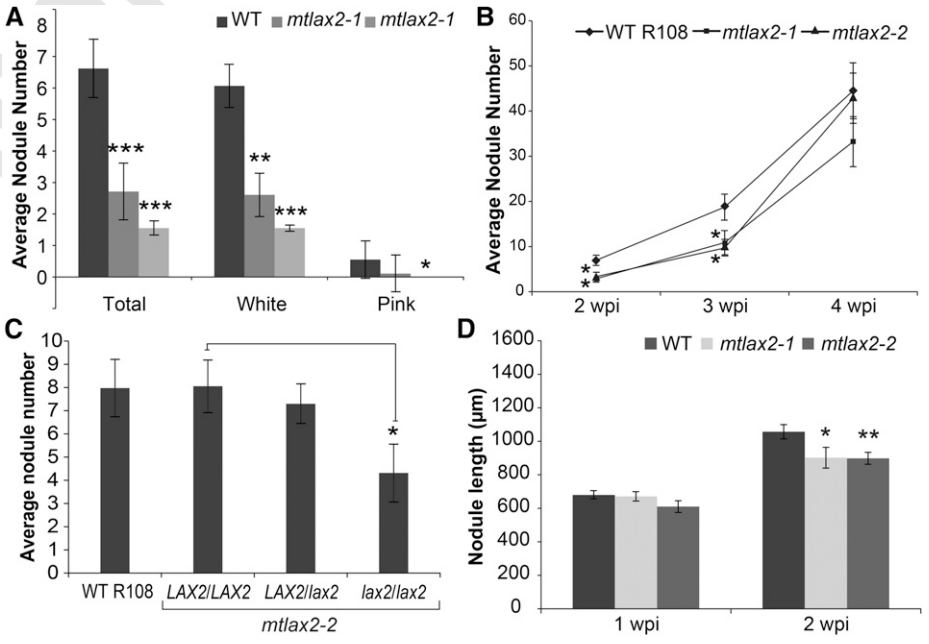

Figure 4. Nodulation phenotypes of *mtlax2* mutants. A, Numbers of pink and white nodules on the *mtlax* mutants 1 wpi with *S. meliloti* (Rm1021). Student's *t* test $*P < 0.05$, $**P < 0.01$, $***P < 0.001$; n = 29, 28, and 29 for control *mtlax2-1* and *mtlax2-2*, respectively. Bars depict SEM. B, Average nodule number on wild type (R108) compared to *mtlax2-1* and *mtlax2-2* mutants 2 to 4 wpi with *S. meliloti* (Rm1021). Student's *t* test, $*P \leq 0.05$; n = 17–22. Bars represent SEM. C, Average nodule number for different genotypes in a population segregating for *mtlax2-2* compared to wild type (WT) (R108). Student's *t* test $*P < 0.05$; n = 38, 38, 83, and 19, respectively. D, Average nodule length on wild type and *mtlax2* alleles inoculated with *S. meliloti*. Student's *t* test $*P < 0.05$ and $**P < 0.01$. For 1 wpi, n = 46, 49, and 31 and 2 wpi, n = 51, 24, and 55 for wild type, *mtlax2-1*, and *mtlax2-2*. Bars represent SEM.

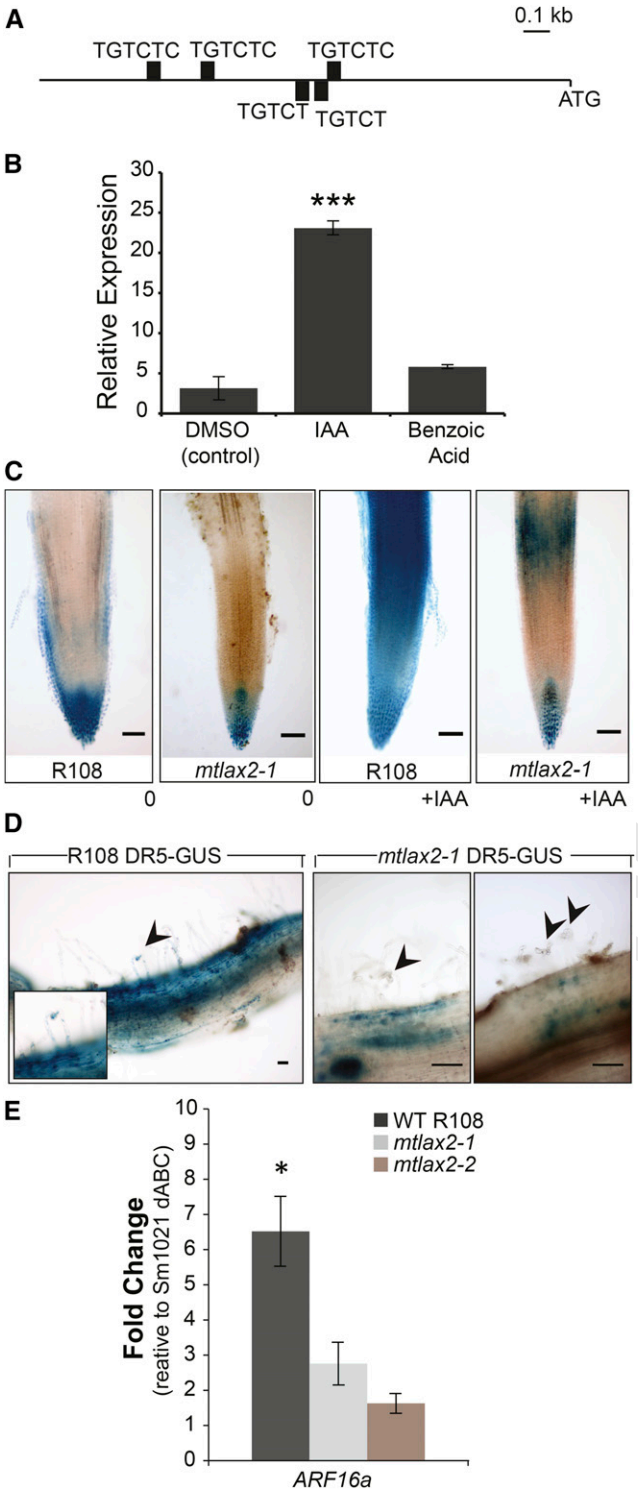

Figure 5. *mtlax2-1* shows aberrant auxin responses. A, Three full auxin responsive elements (TGTCTC) and two TGTCT motifs are present in the 2-kb promoter region of *MtLAX2*. B, Expression of *MtLAX2* in *M. truncatula* roots upon a 3-h treatment with IAA (1 μM) or its structural analog benzoic acid (BA; 1 μM), as measured by qRT-PCR. Data are average of three biological replicates consisting of eight seedlings each. Student's *t* test ***$P < 0.001$. C, Comparison of wild type (WT) (R108) and *mtlax2-1* carrying the *DR5-GUS* reporter with and without IAA treatment. The *mtlax2* mutant exhibits less GUS staining than wild type (R108), and this difference is enhanced after treatment with 1 μM IAA. Scale bars represent 100 μM. D, Representative images of *mtlax2-1* and wild-type soil-grown seedlings with the *DR5-GUS* reporter 2 dpi with Rm1021. The *mtlax2-1* mutant shows reduced *DR5-GUS* staining in the vicinity of infected root hairs (arrowheads) compared to wild type (R108). Scale bars represent 100 μM. E, Expression of *ARF16a* in the wild type and *mtlax2* mutant backgrounds 2 dpi with Rm1021 relative to controls inoculated with SL44 (*S. meliloti nodΔD1ABC*) using qRT-PCR. Student's *t* test *$P < 0.05$, **$P < 0.01$. Three to four biological replicates were used per genotype each consisting of five seedlings each. Expression values were normalized using *UBIQUITIN* and *TIP41*.

observed expression of *MtLAX2* in nodules was dependent on legume-specific cis elements, we analyzed a transgenic *Pisum sativum* GUS reporter line (*AtAUX1*$_{pro}$-*GUS*) in which the GUS gene was driven by the Arabidopsis *AUX1* promoter. This analysis revealed expression throughout the nodule primordia and at the nodule apex, a similar pattern to that of *MtLAX2* (Supplemental Fig. S8, A–C). [AU : 8]

MtLAX2 is predicted to increase intracellular auxin levels and thereby increase auxin signaling in those cells. To test this hypothesis, we crossed *mtlax2-1* to a transgenic line carrying the *DR5-GUS* auxin reporter. In wild-type seedlings, auxin-regulated GUS reporter staining was strong throughout root apical meristems and in epidermal cells above the root apex (Fig. 5C, first). In *mtlax2*, the staining was much less than wild type and was predominantly limited to the root tip columella tissues with weak staining in neighboring cells (Fig. 5C, second). In seedlings treated with 1 μM IAA for 3 h, wild type (as expected) showed increased staining due to *DR5-GUS*; an increase was also seen in the *mtlax2-1* mutant, but the increase was much less than that seen in wild type (Fig. 5C, third and fourth). We therefore conclude that auxin signaling in *mtlax2* roots is strongly reduced.

MtLAX2 Is Required for Auxin Signaling Responses during Early Stages of Nodulation

During nodulation, the *DR5-GUS* marker accumulates in root hairs undergoing infection (Breakspear et al., 2014). Using the DR5 reporter as a readout of the auxin signaling pathway, we used the *mtlax2-1 DR5-GUS* line to query whether early hormone responses at sites of nodule formation were altered relative to the wild-type control. Seven-day-old seedlings were infected with *lacZ*-marked *S. meliloti* and differentially stained for β-galactosidase (LacZ) and GUS activity 2 d postinoculation (dpi). The number of infection events associated with *DR5-GUS* staining was reduced in the *mtlax2* mutant (wild type = 9.7 $\pm$ 1.50 [SEM] infections/plant, *mtlax2-1*=2.1 $\pm$ 0.5, $P = 0.0006$, Student's *t* test, $n = 10$ for wild type and $n = 17$ for *mtlax2-1*). In addition, in comparison to wild type, the extent of GUS staining in the vicinity of infections was reduced in *mtlax2-1* (Fig. 5D).

To further investigate the role of MtLAX2 in auxin responses during nodulation, we tested the expression of the early auxin responsive gene *Auxin Response Factor 16a* (*ARF16a*), which is highly expressed in emerging nodules and in infected root hairs (Breakspear et al., 2014). Seven-day-old seedlings were inoculated with Rm1021, and the root tissue was harvested at 2 dpi. To improve sensitivity, the lateral and primary root tips were removed since *ARF16a* is highly expressed in these tissues. *ARF16a* transcript levels were then monitored using qRT-PCR. A significant increase in *ARF16a* levels in response to rhizobial inoculation was observed in wild type but not in the *mtlax2* mutants, suggesting that accumulation of auxin signaling genes at sites of infection require the auxin influx carrier MtLAX2 (Fig. 5E). Promoter-GUS analysis of *ARF16a* shows its expression strongly overlaps with that of *MtLAX2* and [AU : 9] both are expressed in the nodule primordia, the nodule vascular bundle, and the apex of mature nodules (Supplemental Fig. S9; Breakspear et al., 2014). However, *ARF16a* is strongly expressed in infected epidermal cells (Breakspear et al., 2014), a pattern that we did not observe for *MtLAX2*, indicating that the two genes are at least in part differentially regulated. Expression of two other infection-induced auxin responsive markers identified in Breakspear et al., 2014, *MtGH3.1* and *MtIAA9* (Supplemental Fig. S6E), show a similar expression pattern to that of *MtARF16a* and appear to have higher expressions in wild type compared to *mtlax2-1* and *mtlax2-2* upon infection. However, these differences were not statistically significant in the three replicates. This might be because these transcripts appear to be most highly induced in nodules and root hairs.

DISCUSSION

The plant hormone auxin represents a critical signal during root growth and development. The AUX/LAX family of auxin influx transporters, including AUX1 and LAX3, have been shown to play key roles during primary and lateral root development (Bennett et al., 1996; Marchant et al., 2002; Swarup et al., 2008). We report that MtLAX2 plays an important role in the formation of root nodules and lateral roots in legumes, indicating common requirements for auxin influx activity for both forms of lateral organs.

During nodulation, *MtLAX2* was expressed in the cortex below sites of rhizobial infection and in the developing nodule primordium. The latter finding is consistent with the report by de Billy et al. (2001), where in situ hybridization was used to study *LAX* gene expression. In mature nodules, expression was limited to the nodule apex, including the meristem and the distal infection zone. Expression was also seen in nodule vascular tissues in developing nodules. Nonsymbiotic expression of *MtLAX2* was seen in root tips, lateral root primordia, and vascular tissues, matching the patterns observed for Arabidopsis *AUX1* (Swarup et al., 2001; Péret et al., 2012). Phylogenetic and synteny analyses indicate that *MtLAX2* is paralogous to *AtAUX1* and in support of this, *MtLAX2* has the same gene structure consisting of eight exons, a feature that distinguishes *AtAUX1* and *AtLAX1* from the *AtLAX2*/*AtLAX3* clade (Swarup, and Péret, 2012). The *ataux1* and *mtlax2* mutants have highly similar phenotypes, including decreased primary root growth, fewer lateral roots, decreased gravitropic growth, shorter root hairs, and auxin resistance, indicating they are functionally analogous. It appears therefore that *MtLAX2* was recruited into nodulation from the existing root development pathway. This is similar to genes such as the *PLT*s that are not symbiosis specific but are further involved in root developmental programs (Franssen et al., 2015). However, the gravitropic growth and the root hair elongation phenotypes of the *mtlax2* mutants are less severe than observed for Arabidopsis *aux1* mutants (Pitts et al., 1998; Fig. 3). This may be due to functional redundancy in *M. truncatula*, possibly with the close homolog *MtLAX1*, which is expressed at similar or higher levels than *MtLAX2* in the root (*Medicago* Gene Atlas; Benedito et al., 2008; de Billy et al., 2001). Despite good expression, the *AtAUX1pro-MtLAX2* transgene failed to complement *ataux1-22*. It was reported previously that *aux1* could not be complemented by other Arabidopsis LAX family members due to improper intracellular trafficking of these proteins in cell types normally expressing AUX1 (Péret et al., 2012). We propose that while MtLAX2 and AtAUX1 are paralogues and are functional analogs in the context of root development, they have acquired differences at the amino acid level that have caused them to be biochemically inequivalent.

qRT-PCR data show that absence of MtLAX2 interferes with early induction of the gene encoding the ARF16a transcription factor (Fig. 5D). The reduced expression of *ARF16a* may be a direct consequence of decreased auxin accumulation in cells of the nodule primordia in *lax2* mutants. Members of the ARF family have been shown to bind to AREs (AUXIN RESPONSE ELEMENTS) to promote (ARF activators) or repress (ARF repressors) gene expression (Ulmasov et al., 1997, 1999; reviewed by Li et al., 2016). Several ARF family members are expressed in mature nodules (Roux et al., 2014). These ARFs, which include eight predicted ARF activators, are expressed in a gradient across the nodule zones, with the highest expression seen in the nodule apex (meristem, distal infection zone), coincident with expression of cyclin genes (data from Roux et al., 2014; summarized in Murray, 2016). The strong overlap of *MtLAX2* expression with auxin signaling genes such as *ARF16a* and cell division markers in the nodule apex is consistent with auxin's role in cell division; mutations in *MtLAX2* resulted in slower growing nodules (Fig. 4, A–D). Furthermore, *MtLAX2* expression was found to be strongly induced by exogenous IAA, consistent with the presence of several AREs in the *MtLAX2* promoter. This is supported by the recent findings of Herrbach et al. (2017) who reported that *MtLAX2* is induced by

the auxin analog 1-naphthaleneacetic acid, but not by the application of Nod factors. In Arabidopsis, two studies found *AtAUX1* to be auxin inducible (Paponov [AU : 10] et al., 2008; Vanneste et al., 2005), but this induction was not seen in a later study (Péret et al., 2012). The strong inducibility of *MtLAX2* by auxin, and the fact that the *AtAUX1* promoter was functional in pea nodules, opens the possibility that regulation of *MtLAX2* in nodulation could be, at least in part, regulated by auxin.

The expression of AUX1 orthologs has been studied using promoter-GUS assays in two actinorhizal plants: *Casuarina glauca*, which forms infection threads in curled root hairs, and *Discaria trinervis*, which does not form infection threads. The reported pattern of expression for the promoter of *DtAUX1* in *D. trinervis* [AU : 11] (Imanishi et al., 2014) is similar to what we find for *MtLAX2* of in *M. truncatula*, with expression in the nodule meristem but not in nodule infected cells. Intriguingly, the *CgAUX1* promoter gave the same pattern of expression in *D. trinervis*, despite its very different pattern of expression in *C. glauca*, where it was expressed in infected root hair cells and infected cells of the nodule but not in the nodule primordium (Péret et al., 2007). This indicates that regulation of *AUX1* homologs is host specific. However, despite clear evidence for activation of auxin signaling in *M. truncatula* root hairs (Breakspear et al., 2014), we did not observe expression of *MtLAX2* in epidermal cells containing infection threads. Together, these results suggest that while presumably important, the presence of auxin itself is not sufficient to activate all auxin responsive genes in a given tissue/cell type. Instead, specific activation of gene expression could vary depending on which auxin signaling module is activated, as has been reported for lateral root development (Goh et al., 2012). Based on these results we suggest that LAX2's role in the enhancement of auxin signaling in infected root hairs is indirect.

Expression of *MtLAX2* at the site of primordia formation and in the nodule meristem implicate MtLAX2 in localized accumulation of auxin at these sites. However, it cannot be excluded that MtLAX2 effects on nodulation are also partly through its expression in other tissues. A role has been demonstrated for AtAUX1 in leaf vascular tissues for shoot-root long distance auxin transport contributing to lateral root formation and *MtLAX2* is also expressed in leaves (*Medicago* Gene Atlas; Marchant et al., 2002). Similarly, MtLAX2 activity in aerial tissues may contribute to the shoot-to-root loading of auxin, resulting in lower auxin responses in *mtlax2* roots as evidenced by the decreased expression of DR5-GUS in the mutant (Fig. 5B).

Over the last decade and a half, numerous studies using auxin markers point to a central role for this hormone in nodulation. Advancement of our understanding of nodule development will require an understanding of how these changes in auxin distribution and signaling are achieved. Here we have demonstrated the requirement for MtLAX2 in the auxin responses associated with rhizobial infection and subsequent nodule formation. However, in addition to auxin influx, auxin efflux has also been shown to be important for nodulation and lateral root formation (Huo et al., 2006; Marhavý et al., 2013; Benková et al., 2003). In lateral root formation, a model has been proposed in which the auxin efflux carrier PIN3 channels auxin to the pericycle founder cell prior to the initial division (Marhavý et al., 2013). It is possible that LAXs and PINs similarly cooperate to increase auxin levels to initiate the divisions leading to nodule formation. Candidates for this role are *MtPIN2*, *MtPIN3*, and *MtPIN4*, which, when knocked down, result in reduced nodule number (Huo et al., 2006). But is auxin required to trigger the first divisions of nodule initiation? Normally, nodules form only at sites associated with successful rhizobial infections, but in mutants with gain-of-function alleles in either components of Nod factor signaling, or in cytokinin perception, nodules spontaneously form in the absence of rhizobia (Tirichine et al., 2006, 2007; Singh et al., 2014; Gleason et al., 2006). This indicates that the site of nodule formation is determined by the plant, and that Nod factor signaling is directly upstream of the events leading to auxin accumulation and cell divisions. Indeed, increased expression of auxin markers is associated with spontaneous nodule formation (Suzaki et al., 2012), and we have shown a strong inhibition of nodule formation by NPA, confirming earlier work (Prayitno et al., 2006; Takanashi et al., 2011a). In contrast, transient treatment with high concentrations of NPA can induce the formation of nodule-like structures, so-called pseudonodules (Allen et al., 1953; Hirsch et al., 1989; Rightmyer and Long, 2011). Furthermore, inoculation of legume roots with rhizobia causes inhibition of polar auxin transport (Boot et al., 1999; Prayitno et al., 2006; Mathesius et al., 2006), suggesting that an interruption of auxin flow [AU : 12] may be required for nodule formation in indeterminate nodules. Evidence suggests that flavonoids, which appear to act as inhibitors of auxin efflux, may mediate localized inhibition of auxin transport during nodulation (Jacobs and Rubery, 1988; Mathesius et al., 1998; Brown et al., 2001; Wasson et al., 2006), and it has been shown that this phenomena is dependent on the cytokinin receptor CRE1 and flavonoid biosynthesis (Plet et al., 2011). Moreover, flavonoids and other auxin transport inhibitors can rescue nodulation in *cre1* mutants, indicating that flavonoids act downstream of cytokinin signaling to modulate auxin transport (Ng et al., 2015). Fitting with this model, flavonoids are produced at higher levels in the root hair differentiation zone where nodules form (Djordjevic et al., 1987; Peters and Long, 1988), and key flavonoid biosynthetic genes are specifically upregulated in nascent nodule primordia (Breakspear et al., 2014; Liu et al., 2015). One pos- [AU : 13] sible scenario is that flavonoid production below infection sites causes localized auxin accumulation, which further leads to increased expression of *MtLAX2*, increasing auxin levels and leading to nodule formation. This work, through identification of LAX2, advances our understanding of the events leading to

changes in auxin accumulation in nodulation and provides an essential tool to conduct future studies to understand hormone interactions during nodulation.

MATERIALS AND METHODS

Plant Growth Conditions and Nodulation Assays

Medicago truncatula ecotypes Jemalong A17, Jester A17, and R108 seedlings were used in this study. All mutants and transgenic plants described were derivatives of either ecotype. Plants were grown in a 1:1 mixture of terragreen and sharp sand or in John Innes Cereal Mix (loam based). Plants were watered regularly as needed and kept in controlled environment chambers with a 16-h photoperiod at 20°C and 80% humidity. For nodulation assays, germinated seedlings were transferred to 4-cm-diameter pots filled with sterile 1:1 mixture of terragreen and sharp sand, and seedlings were allowed to grow for 1 week before inoculation. *Sinorhizobium meliloti* Rm1021 was inoculated at the base of each seedling using a 1-mL suspension (OD_{600} between 0.02 and 0.05 in water) added after 1 week after germination, and nodules were counted at different time points. The spot inoculation technique is described separately below.

Inhibitor Treatment and Rhizobial Infection Assays

Seedlings were either grown on distilled water agar or basic nodulation medium (BNM) using a filter paper sandwich method as described (Breakspear et al., 2014). Seedlings were grown vertically on 1.5% agarose slants between two filter paper squares. The required volume of chemical in the solvent carrier was mixed in 50 mL of melted agarose medium per plate. For the infection assays, germinated seedlings were pretreated on the inhibitor-containing medium for 24 h before inoculation with 1 mL of *lacZ*-marked *S. meliloti* Rm2011 suspension as above. Seedlings were then grown for 7 d at 25°C in controlled environment chambers with a 16-h photoperiod, histochemically stained using X-gal and X-gluc, and infection threads were scored by light microscopy (Nikon Eclipse 800).

Calcium Spiking Measurements

Analysis of calcium spiking was done in the presence of the chemicals and 1×10^{-9} M Nod factor as described previously (Sun et al., 2015).

Spot Inoculation and Auxin Treatment of *M. truncatula* Roots

Jester A17 seeds were grown for 2 d on BNM medium supplemented with [AU : 14] 1 μM aminoethoxyvinyl-Gly (Sigma) at 22°C 16L/8D. *S. meliloti* 2011 was grown in minimal medium supplemented with 3 μM luteolin (Sigma) and diluted to a final concentration 0.02 OD_{600nm} using Fahraeus plant medium. The mock treatment consisted of Fahraeus plant medium with luteolin added and then diluted the same as the inoculant. Approximately 1 μL of the *S. meliloti* suspension or mock treatment was inoculated onto the infection zone, and 16 h later, these were dissected as 2- to 3-mm segments. About 50 to 60 segments were collected per biological replicate, frozen in liquid nitrogen, and stored at −80°C. RNA was extracted using the RNeasy Micro Kit (Qiagen), and cDNA was prepared from 0.5 μg total RNA using iSCRIPT cDNA SYNTHESIS KIT according to the manufacturer's instructions (Bio-Rad).

For treatment with auxin, overnight-germinated seedlings were grown on water-agarose medium for 3 d. Eight plants per replicate were transferred for 3 h to small petri dishes containing liquid BNM containing 1 μM IAA or the solvent control. Root tips of the treated seedlings were removed, and only the root zone with root hairs was collected for RNA extraction.

RNA Purification from Roots and Quantitative PCR

RNA was isolated using RNeasy plant mini kit (QIAgen) following the manufacturer's protocol. The eluted RNA was treated with DNase (Ambion) and the quality evaluated by agarose gel electrophoresis. Then 1 μg of total RNA was used for cDNA synthesis using Superscript III (Invitrogen). These cDNA samples were diluted 20-fold in sterile double distilled water. Forward and reverse primers were added at a final concentration of 0.2 mM, to which 5 μL of the diluted cDNA and 10 μL of SYBR Green Taq Ready Mix (Sigma) were added, making a reaction volume of 20 μL. A minimum of three biological replicates was used per treatment and qPCR reactions performed using the Biorad CFX96 real-time system.

Gene Cloning

A 2,983-bp fragment upstream of *MtLAX2* start site was amplified from *M. truncatula* A17 genomic DNA using Phusion High-Fidelity DNA Polymerase (NEB). The fragments were cloned into pDONR201 using Gateway BP Clonase II enzyme mix (Invitrogen) and recombined into the pKGWFS7 Gateway destination vector by LR reaction to create $MtLAX2_{pro}$-*GUS*. For cloning the MtLAX2 cDNA, the 1,455-bp coding region was PCR amplified from a root cDNA library as described above. The primers used in this study are listed in Supplemental Table S1 (Primers).

Generation of Stably Transformed Hairy Root Lines of *M. truncatula*

Plant roots transformed with promoter-GUS constructs were generated in *M. truncatula* A17 background by hairy root transformation as described (Breakspear et al., 2014). The composite plants were transferred to water agar with 100 nM aminoethoxyvinyl-Gly or to a mixture of equal amounts of sand and terragreen 4 weeks after transformation. The roots were then inoculated with Rm2011 pXLGD4 (*lacZ*). The roots were harvested at different time points for GUS staining, and some samples were then stained with Magental-gal (Melford) for visualization of Rm2011 pXLGD4 as previously reported (Pichon et al., 1994). [AU : 15]

Generation of *Pisum sativum* AtAUX1-GUS Transgenic Lines

The AtAUX1-GUS construct (Marchant et al., 1999) was transformed into *P. sativum* using *Agrobacterium tumefaciens*. Transgenic shoots were selected using 5 μg/mL phosphinothricin, grafted onto wild-type shoots, and allowed to set seed. These lines were also confirmed by a PCR reaction for presence of *AtAUX1:GUS*. The copy number of the Bar gene was analyzed by Southern blot as described by Sambrook et al. (1989). Lines homozygous for the construct were propagated and seedlings of the progeny analyzed.

Histochemical GUS Assays

GUS staining was performed in 50 mM sodium phosphate buffer (pH 7.0) containing 1 mg/mL X-Gluc (Melford), 1 mM EDTA, and 1% Triton-X100. Samples were stained overnight and then washed with fresh buffer before imaging. For sectioning, nodule samples were fixed in 2.5% gluteraldehyde and left overnight in 30% Suc. Sections were made using the cryostar NX70 (Thermo Scientific) and images taken with a Nikon Eclipse E800 light microscope.

mtlax2-1 DR5-GUS Lines

DR5-GUS expression was analyzed using a stably transformed line of R108 (Zhou et al., 2011; Guan et al., 2013). The DR5 marker was crossed into the [AU : 16] *mtlax2-1* mutant allele by hand pollination as described in the *Medicago truncatula* handbook.

Insertional Mutant Screening and Genotyping

Tnt1 retrotransposon insertions in *MtLAX2* were screened using a nested PCR approach (Cheng et al., 2011, 2014) selecting for lines with insertions in [AU : 17] exons. R2 progeny were genotyped using primers MtLAX2_Tnt_F and TntR for the *mtlax2-1* (NF14494) and *mtlax2-2* (NF16662) alleles (Supplemental Table S1). PCR reactions were performed using the Go Taq Green Mastermix (Promega).

Phylogenetic Tree Construction

Amino acid sequences for MtLAX1-MtLAX5 were originally described by Schnabel and Frugoli (2004). Gene model and accession numbers are provided in Supplemental Table S2. Phylogenetic analysis was done using Phylogeny.fr

suite of programs as follows (Dereeper et al., 2008). Amino acid sequences were aligned using MUSCLE 3.7 and refined using Gblocks 0.91b. The phylogenetic tree was created using PhyML 3.0 and the tree was rendered using TreeDyn 198.3.

Root Hair and Nodule Length Measurement

Root hair length was measured using the Leica DFC 420 stereo microscope. Five germinated seedlings of *M. truncatula* per plate per treatment were placed between filter paper sandwiches on square petri dishes. The seedlings were grown for 7 d under long days (16 h). To measure the root hair length, the top filter paper was removed with forceps without moving the roots and placed under the microscope. Five consecutive root hairs on each side of the root were measured from the base to the tip of the hair using the Leica application suite Version 4.2.0 software. Nodule length was measured similarly from tip to base after straightening them out to the same plane.

Bacterial Growth

S. meliloti Rm2011 *hemA:lacZ* (Plasmid pXLGD4) was grown overnight in TY medium with appropriate antibiotics, the OD_{600} was measured, and the CFU (colony forming units) calculated. This culture was diluted in fresh TY medium to 10^{-5} CFU. In a 48-well plate, 360 μL of sterile TY medium was added to 40 μL of the diluted culture containing the desired dilution of the chemical to be tested. A minimum of 5 replicates was used per treatment and the wells were randomly assigned per treatment. The plate was shaken at 28°C in an Infinite 2000 plate reader measuring OD600 at hour intervals for up to 70 h. The data were analyzed using Microsoft Excel 2010.

Mycorrhizal Colonization Assay

Seedlings were germinated as described above and then transferred to pots containing equal parts terra green and sand mixed with nurse inoculum containing roots of chive (*Allium schoenoprasum*) plants infected with spores of the mycorrhizal fungus *Rhizophagus irregularis*. Plants were allowed to grow for 4 to 5 weeks before harvesting the root tissue. Roots were then washed and a root sample was collected for analysis. The fungus was visualized using an ink staining protocol (Q. Zhang et al., 2010) and quantified using the grid intersection method (McGonigle et al., 1990).

Complementation Assay

For genetic complementation of *aux1*, *MtLAX2* cDNA was PCR amplified and fused with the Arabidopsis *AUX1* promoter (1.7 kb) and terminator (0.3 kb) in pORFLAUX1 (Péret et al., 2012) between *Xho*I and *Bam*HI sites to create the plasmid pAML2. pAML2 was sequenced to check for PCR errors. Transformation of *A. tumefaciens* (C58) and the Arabidopsis *aux1-22* mutant was done as previously described (Péret et al., 2012). Over 40 independent lines were checked for rescue of *aux1* gravitropism and 2,4-D resistance phenotypes. For these assays, seeds were directly plated on Murashige and Skoog agar plates (1× Murashige and Skoog salts + 1% Suc). For the resistance assay, different levels of 2,4-D were added to the media. The seeds were vernalized overnight and were then grown for 5 d in continuous light before images were taken.

Synteny Analysis

Homology between the Arabidopsis *AUX1* region (obtained from the TAIR database) and regions containing *M. truncatula* LAX genes (genome version MtV4.0) were made using BLAST searches. The NCBI gene accessions are as follows: Medtr5g082220.2 (AY115841.1), Medtr7g067450.1 (AY115843.1), Medtr3g072870.1 (AY115842.1), Medtr4g415390.2 (AY115844.1), and Medtr4g073770.1 (AY115845.1).

Accession Numbers

Sequence data from this article can be found in the GenBank/EMBL data libraries under accession numbers ■■■.

Supplemental Data

The following supplemental data are available.

Supplemental Figure S1. Effect of auxin and auxin influx inhibitors on root growth and nodulation in *M. truncatula*.

Supplemental Figure S2. *MtLAX2* and *AtAUX1* are paralogues.

Supplemental Figure S3. Expression pattern of *MtLAX2*.

Supplemental Figure S4. *mtlax2-1* and *mtlax2-2* mutations result in mis-spliced transcripts containing premature stop codons.

Supplemental Figure S5. *MtLAX2* does not restore *aux1* mutant phenotype.

Supplemental Figure S6. RT-PCR confirmation of *ataux1-22* lines complemented with *MtLAX2*.

Supplemental Figure S7. Symbiotic phenotypes of *mtlax2* mutants.

Supplemental Figure S8. GUS staining in nodules of *P. sativum* stably transformed with AtAUX1pro:GUS.

Supplemental Figure S9. Dynamic expression pattern of *ARF16a* during nodule development.

Supplemental Table S1. List or primers used in this study. All sequences are provided in the 5′ to 3′ orientation.

Supplemental Table S2. Gene identifiers and accession numbers for AUX-LAX genes mentioned in this study.

ACKNOWLEDGMENTS

The authors thank Dr. Elaine Barclay for the nodule sections, Mr. Andrew Davis for nodule photographs, the JIC greenhouse staff for taking care of the plants, and Vinod Kumar for comments on the manuscript.

Received October 11, 2016; accepted March 25, 2017; published March 31, 2017.

LITERATURE CITED

Aida M, Beis D, Heidstra R, Willemsen V, Blilou I, Galinha C, Nussaume L, Noh YS, Amasino R, Scheres B (2004) The *PLETHORA* genes mediate patterning of the *Arabidopsis* root stem cell niche. Cell **119:** 109–120

Allen EK, Allen ON, Newman AS (1953) Pseudonodulation of leguminous plants induced by 2-bromo-3,5- dichlorobenzoic acid. Am J Bot **40:** 429–435

Bean SJ, Gooding PS, Mullincaux PM, Davies DR (1997) A simple system for pea transformation. Plant Cell Rep **16:** 513–519

Benedito VA, Torres-Jerez I, Murray JD, Andriankaja A, Allen S, Kakar K, Wandrey M, Verdier J, Zuber H, Ott T, et al (2008) A gene expression atlas of the model legume *Medicago truncatula*. Plant J **55:** 504–513

Benková E, Michniewicz M, Sauer M, Teichmann T, Seifertová D, Jürgens G, Friml J (2003) Local, efflux-dependent auxin gradients as a common module for plant organ formation. Cell **115:** 591–602

Bennett MJ, Marchant A, Green HG, May ST, Ward SP, Millner PA, Walker AR, Schulz B, Feldmann KA (1996) *Arabidopsis AUX1* gene: a permease-like regulator of root gravitropism. Science **273:** 948–950

Boot KJM, van Brussel AAN, Tak T, Spaink HP, Kijne JW (1999) Lipochitin oligosaccharides from *Rhizobium leguminosarum* bv. viciae reduce auxin transport capacity in *Vicia sativa* subsp nigra roots. Mol Plant Microbe Interact **12:** 839–844

Breakspear A, Liu C, Roy S, Stacey N, Rogers C, Trick M, Morieri G, Mysore KS, Wen J, Oldroyd GE, et al (2014) The root hair "infectome" of *Medicago truncatula* uncovers changes in cell cycle genes and reveals a requirement for Auxin signaling in rhizobial infection. Plant Cell **26:** 4680–4701

Brown DE, Rashotte AM, Murphy AS, Normanly J, Tague BW, Peer WA, Taiz L, Muday GK (2001) Flavonoids act as negative regulators of auxin transport in vivo in *Arabidopsis*. Plant Physiol **126:** 524–535

Casimiro I, Marchant A, Bhalerao RP, Beeckman T, Dhooge S, Swarup R, Graham N, Inzé D, Sandberg G, Casero PJ, et al (2001) Auxin transport promotes *Arabidopsis* lateral root initiation. Plant Cell **13:** 843–852

Couzigou JM, Zhukov V, Mondy S, Abu el Heba G, Cosson V, Ellis TH, Ambrose M, Wen J, Tadege M, Tikhonovich I, et al (2012) *NODULE ROOT* and *COCHLEATA* maintain nodule development and are legume orthologs of *Arabidopsis BLADE-ON-PETIOLE* genes. Plant Cell **24:** 4498–4510

[AU : 25]

de Billy F, Grosjean C, May S, Bennett M, Cullimore JV (2001) Expression studies on *AUX1*-like genes in *Medicago truncatula* suggest that auxin is required at two steps in early nodule development. Mol Plant Microbe Interact **14:** 267–277

De Smet I, Tetsumura T, De Rybel B, Frei dit Frey N, Laplaze L, Casimiro I, Swarup R, Naudts M, Vanneste S, Audenaert D, et al (2007) Auxin-dependent regulation of lateral root positioning in the basal meristem of *Arabidopsis.* Development **134:** 681–690

Delbarre A, Müller P, Imhoff V, Guern J (1996) Comparison of mechanisms controlling uptake and accumulation of 2,4-dichlorophenoxy acetic acid, naphthalene-1-acetic acid, and indole-3-acetic acid in suspension-cultured tobacco cells. Planta **198:** 532–541

Dereeper A, Guignon V, Blanc G, Audic S, Buffet S, Chevenet F, Dufayard JF, Guindon S, Lefort V, Lescot M, et al (2008) Phylogeny.fr: robust phylogenetic analysis for the non-specialist. Nucleic Acids Res **36:** W465-9

Djordjevic MA, Redmond JW, Batley M, Rolfe BG (1987) Clovers secrete specific phenolic compounds which either stimulate or repress nod gene expression in *Rhizobium trifolii.* EMBO J **6:** 1173–1179

Dubrovsky JG, Sauer M, Napsucialy-Mendivil S, Ivanchenko MG, Friml J, Shishkova S, Celenza J, Benková E (2008) Auxin acts as a local morphogenetic trigger to specify lateral root founder cells. Proc Natl Acad Sci USA **105:** 8790–8794

Franssen HJ, Xiao TT, Kulikova O, Wan X, Bisseling T, Scheres B, Heidstra R (2015) Root developmental programs shape the *Medicago truncatula* nodule meristem. Development **142:** 2941–2950

Gleason C, Chaudhuri S, Yang T, Muñoz A, Poovaiah BW, Oldroyd GE (2006) Nodulation independent of rhizobia induced by a calcium-activated kinase lacking autoinhibition. Nature **441:** 1149–1152

Goh T, Kasahara H, Mimura T, Kamiya Y, Fukaki H (2012) Multiple AUX/IAA – ARF modules regulate lateral root formation: the role of *Arabidopsis* SHY2/IAA3-mediated auxin signaling. Phil. Trans. R. Soc **B367:** 1461–1468

Gonzalez-Rizzo S, Crespi M, Frugier F (2006) The *Medicago truncatula* CRE1 cytokinin receptor regulates lateral root development and early symbiotic interaction with *Sinorhizobium meliloti.* Plant Cell **18:** 2680–2693

Guan D, Stacey N, Liu C, Wen J, Mysore KS, Torres-Jerez I, Vernié T, Tadege M, Zhou C, Wang ZY, et al (2013) Rhizobial infection is associated with the development of peripheral vasculature in nodules of *Medicago truncatula.* Plant Physiol **162:** 107–115

Guinel FC (2015) Ethylene, a hormone at the center-stage of nodulation. Front Plant Sci **6:** 1121

Hanlon MT, Coenen C (2011) Genetic evidence for auxin involvement in arbuscular mycorrhiza initiation. New Phytol **189:** 701–709

Heidstra R, Yang WC, Yalcin Y, Peck S, Emons AM, van Kammen A, Bisseling T (1997) Ethylene provides positional information on cortical cell division but is not involved in Nod factor-induced root hair tip growth in Rhizobium-legume interaction. Development **124:** 1781–1787

Herrbach V, Remblière C, Gough C, Bensmihen S (2014) Lateral root formation and patterning in *Medicago truncatula.* J Plant Physiol **171:** 301–310

Herrbach V, Chirinos X, Rengel D, Agbevenou K, Vincent R, Pateyron S, Huguet S, Balzergue S, Pasha A, Provart N, et al (2017) Nod factors potentiate auxin signaling for transcriptional regulation and lateral root formation in *Medicago truncatula.* J Exp Bot erw474

Hirsch AM, Bhuvaneswari TV, Torrey JG, Bisseling T (1989) Early nodulin genes are induced in alfalfa root outgrowths elicited by auxin transport inhibitors. Proc Natl Acad Sci USA **86:** 1244–1248

Huo X, Schnabel E, Hughes K, Frugoli J (2006) RNAi phenotypes and the localization of a protein:GUS fusion imply a role for *Medicago truncatula* PIN genes in nodulation. J Plant Growth Regul **25:** 156–165

Jacobs M, Rubery PH (1988) Naturally occurring auxin transport regulators. Science **241:** 346–349

Laskowski M, Grieneisen VA, Hofhuis H, Hove CA, Hogeweg P, Marée AF, Scheres B (2008) Root system architecture from coupling cell shape to auxin transport. PLoS Biol **6:** e307

Lavenus J, Goh T, Roberts I, Guyomarc'h S, Lucas M, De Smet I, Fukaki H, Beeckman T, Bennett M, Laplaze L (2013) Lateral root development in Arabidopsis: fifty shades of auxin. Trends Plant Sci **18:** 450–458

Li SB, Xie ZZ, Hu CG, Zhang JZ (2016) A review of auxin response factors (ARFs) in plants. Front Plant Sci **7:** 47

Lohar D, Stiller J, Kam J, Stacey G, Gresshoff PM (2009) Ethylene insensitivity conferred by a mutated *Arabidopsis* ethylene receptor gene alters nodulation in transgenic *Lotus japonicus.* Ann Bot (Lond) **104:** 277–285

Lucas M, Kenobi K, von Wangenheim D, Voβ U, Swarup K, De Smet I, Van Damme D, Lawrence T, Péret B, Moscardi E, et al (2013) Lateral root morphogenesis is dependent on the mechanical properties of the overlaying tissues. Proc Natl Acad Sci USA **110:** 5229–5234

Malamy JE, Benfey PN (1997) Organization and cell differentiation in lateral roots of *Arabidopsis* thaliana. Development **124:** 33–44

Marchant A, Bhalerao R, Casimiro I, Eklöf J, Casero PJ, Bennett M, Sandberg G (2002) AUX1 promotes lateral root formation by facilitating indole-3-acetic acid distribution between sink and source tissues in the *Arabidopsis* seedling. Plant Cell **14:** 589–597

Marchant A, Kargul J, May ST, Muller P, Delbarre A, Perrot-Rechenmann C, Bennett MJ (1999) AUX1 regulates root gravitropism in Arabidopsis by facilitating auxin uptake within root apical tissues. EMBO J **18:** 2066–2073

Marhavý P, Vanstraelen M, De Rybel B, Zhaojun D, Bennett MJ, Beeckman T, Benková E (2013) Auxin reflux between the endodermis and pericycle promotes lateral root initiation. EMBO J **32:** 149–158

Mathesius U, Schlaman HR, Spaink HP, Of Sautter C, Rolfe BG, Djordjevic MA (1998) Auxin transport inhibition precedes root nodule formation in white clover roots and is regulated by flavonoids and derivatives of chitin oligosaccharides. Plant J **14:** 23–34

McGonigle TP, Miller MH, Evans DG, Fairchild GL, Swan JA (1990) A new method which gives an objective measure of colonization of roots by vesicular—arbuscular mycorrhizal fungi. New Phytol **115:** 495–501

Miri M, Janakirama P, Held M, Ross L, Szczyglowski K (2016) Into the root: how cytokinin controls rhizobial infection. Trends Plant Sci **21:** 178–186

Murray JD, Karas BJ, Sato S, Tabata S, Amyot L, Szczyglowski K (2007) A cytokinin perception mutant colonized by Rhizobium in the absence of nodule organogenesis. Science **315:** 101–104

Murray JD (2016) The cell cycle in nodulation. *In* R Rose, ed, Molecular Cell Biology of the Growth and Differentiation of Plant Cells. Taylor & Francis, CRC Press. doi: 10.1201/b20316

[AU : 26]

Ng JL, Hassan S, Truong TT, Hocart CH, Laffont C, Frugier F, Mathesius U (2015) Flavonoids and auxin transport inhibitors rescue symbiotic nodulation in the *Medicago truncatula* cytokinin perception mutant *cre1.* Plant Cell **27:** 2210–2226

Pacios-Bras C, Schlaman HR, Boot K, Admiraal P, Langerak JM, Stougaard J, Spaink HP (2003) Auxin distribution in *Lotus japonicus* during root nodule development. Plant Mol Biol **52:** 1169–1180

Penmetsa RV, Frugoli JA, Smith LS, Long SR, Cook DR (2003) Dual genetic pathways controlling nodule number in *Medicago truncatula.* Plant Physiol **131:** 998–1008

Péret B, Swarup R, Jansen L, Devos G, Auguy F, Collin M, Santi C, Hocher V, Franche C, Bogusz D, et al (2007) Auxin influx activity is associated with Frankia infection during actinorhizal nodule formation in *Casuarina glauca.* Plant Physiol **144:** 1852–1862

Péret B, Swarup K, Ferguson A, Seth M, Yang Y, Dhondt S, James N, Casimiro I, Perry P, Syed A, et al (2012) AUX/LAX genes encode a family of auxin influx transporters that perform distinct functions during Arabidopsis development. Plant Cell **24:** 2874–2885

Peters NK, Long SR (1988) Alfalfa root exudates and compounds which promote or inhibit induction of *Rhizobium meliloti* nodulation genes. Plant Physiol **88:** 396–400

Pinon V, Prasad K, Grigg SP, Sanchez-Perez GF, Scheres B (2013) Local auxin biosynthesis regulation by PLETHORA transcription factors controls phyllotaxis in *Arabidopsis.* Proc Natl Acad Sci USA **110:** 1107–1112

Pitts RJ, Cernac A, Estelle M (1998) Auxin and ethylene promote root hair elongation in *Arabidopsis.* Plant J **16:** 553–560

Plet J, Wasson A, Ariel F, Le Signor C, Baker D, Mathesius U, Crespi M, Frugier F (2011) MtCRE1-dependent cytokinin signaling integrates bacterial and plant cues to coordinate symbiotic nodule organogenesis in *Medicago truncatula.* Plant J **65:** 622–633

Prayitno J, Rolfe BG, Mathesius U (2006) The ethylene-insensitive *sickle* mutant of *Medicago truncatula* shows altered auxin transport regulation during nodulation. Plant Physiol **142:** 168–180

Rahman A, Hosokawa S, Oono Y, Amakawa T, Goto N, Tsurumi S (2002) Auxin and ethylene response interactions during Arabidopsis root hair development dissected by auxin influx modulators. Plant Physiol **130:** 1908–1917

Rightmyer AP, Long SR (2011) Pseudonodule formation by wild-type and symbiotic mutant *Medicago truncatula* in response to auxin transport inhibitors. Mol Plant Microbe Interact **24:** 1372–1384

Roux B, Rodde N, Jardinaud MF, Timmers T, Sauviac L, Cottret L, Carrère S, Sallet E, Courcelle E, Moreau S, et al (2014) An integrated analysis of plant and bacterial gene expression in symbiotic root nodules using laser-capture microdissection coupled to RNA sequencing. Plant J **77:** 817–837

Sambrook J, Fritsch EF, Maniatis T (1989) Molecular Cloning: A Laboratory Manual. Cold Spring Harbor Laboratory, Cold Spring Harbor, NY.

Schnabel EL, Frugoli J (2004) The PIN and LAX families of auxin transport genes in *Medicago truncatula.* Mol Genet Genomics **272:** 420–432

Singh S, Katzer K, Lambert J, Cerri M, Parniske M (2014) CYCLOPS, a DNA-binding transcriptional activator, orchestrates symbiotic root nodule development. Cell Host Microbe **15:** 139–152

Subramanian S, Stacey G, Yu O (2006) Endogenous isoflavones are essential for the establishment of symbiosis between soybean and *Bradyrhizobium japonicum.* Plant J **48:** 261–273

[**AU : 27**]

Sun J, Miller JB, Granqvist E, Wiley-Kalil A, Gobbato E, Maillet F, Cottaz S, Samain E, Venkateshwaran M, Fort S, et al (2015) Activation of symbiosis signaling by arbuscular mycorrhizal fungi in legumes and rice. Plant Cell **27:** 823–838

Suzaki T, Ito M, Kawaguchi M (2013) Induction of localized auxin response during spontaneous nodule development in *Lotus japonicus.* Plant Signal Behav **8:** e23359

Suzaki T, Yano K, Ito M, Umehara Y, Suganuma N, Kawaguchi M (2012) Positive and negative regulation of cortical cell division during root nodule development in *Lotus japonicus* is accompanied by auxin response. Development **139:** 3997–4006

Swarup K, Benková E, Swarup R, Casimiro I, Péret B, Yang Y, Parry G, Nielsen E, De Smet I, Vanneste S, et al (2008) The auxin influx carrier LAX3 promotes lateral root emergence. Nat Cell Biol **10:** 946–954

Swarup R, Péret B (2012) AUX/LAX family of auxin influx carriers-an overview. Front Plant Sci **3:** 225

Swarup R, Friml J, Marchant A, Ljung K, Sandberg G, Palme K, Bennett M (2001) Localization of the auxin permease AUX1 suggests two functionally distinct hormone transport pathways operate in the Arabidopsis root apex. Genes Dev **15:** 2648–2653

Takanashi K, Sugiyama A, Yazaki K (2011a) Involvement of auxin distribution in root nodule development of *Lotus japonicus.* Planta **234:** 73–81

Takanashi K, Sugiyama A, Yazaki K (2011b) Auxin distribution and lenticel formation in determinate nodule of *Lotus japonicus.* Plant Signal Behav **6:** 1405–1407

Timmers AC, Auriac MC, Truchet G (1999) Refined analysis of early symbiotic steps of the Rhizobium-*Medicago* interaction in relationship with microtubular cytoskeleton rearrangements. Development **126:** 3617–3628

Tirichine L, Imaizumi-Anraku H, Yoshida S, Murakami Y, Madsen LH, Miwa H, Nakagawa T, Sandal N, Albrektsen AS, Kawaguchi M, et al (2006) Deregulation of a Ca2+/calmodulin-dependent kinase leads to spontaneous nodule development. Nature **441:** 1153–1156

Tirichine L, Sandal N, Madsen LH, Radutoiu S, Albrektsen AS, Sato S, Asamizu E, Tabata S, Stougaard J (2007) A gain-of-function mutation in a cytokinin receptor triggers spontaneous root nodule organogenesis. Science **315:** 104–107

Ulmasov T, Hagen G, Guilfoyle TJ (1997) ARF1, a transcription factor that binds to auxin response elements. Science **276:** 1865–1868

Ulmasov T, Hagen G, Guilfoyle TJ (1999) Dimerization and DNA binding of auxin response factors. Plant J **19:** 309–319

Ulmasov T, Liu ZB, Hagen G, Guilfoyle TJ (1995) Composite structure of auxin response elements. Plant Cell **7:** 1611–1623

[**AU : 28**]

Vanneste S, De Rybel B, Beemster GT, Ljung K, De Smet I, Van Isterdael G, Naudts M, Iida R, Gruissem W, Tasaka M, et al (2005) Cell cycle progression in the pericycle is not sufficient for SOLITARY ROOT/IAA14-mediated lateral root initiation in Arabidopsis thaliana. Plant Cell **17:** 3035–3050

van Noorden GE, Ross JJ, Reid JB, Rolfe BG, Mathesius U (2006) Defective long-distance auxin transport regulation in the *Medicago truncatula* super numeric nodules mutant. Plant Physiol **140:** 1494–1506

Walcher CL, Nemhauser JL (2012) Bipartite promoter element required for auxin response. Plant Physiol **158:** 273–282

Wasson AP, Pellerone FI, Mathesius U (2006) Silencing the flavonoid pathway in *Medicago truncatula* inhibits root nodule formation and prevents auxin transport regulation by rhizobia. Plant Cell **18:** 1617–1629

Xiao TT, Schilderink S, Moling S, Deinum EE, Kondorosi E, Franssen H, Kulikova O, Niebel A, Bisseling T (2014) Fate map of *Medicago truncatula* root nodules. Development **141:** 3517–3528

Yamaguchi N, Jeong CW, Nole-Wilson S, Krizek BA, Wagner D (2016) AINTEGUMENTA and AINTEGUMENTA-LIKE6/PLETHORA3 induce *LEAFY* expression in response to auxin to promote the onset of flower formation in *Arabidopsis.* Plant Physiol **170:** 283–293